SUPPLEMENTAL FIGURES

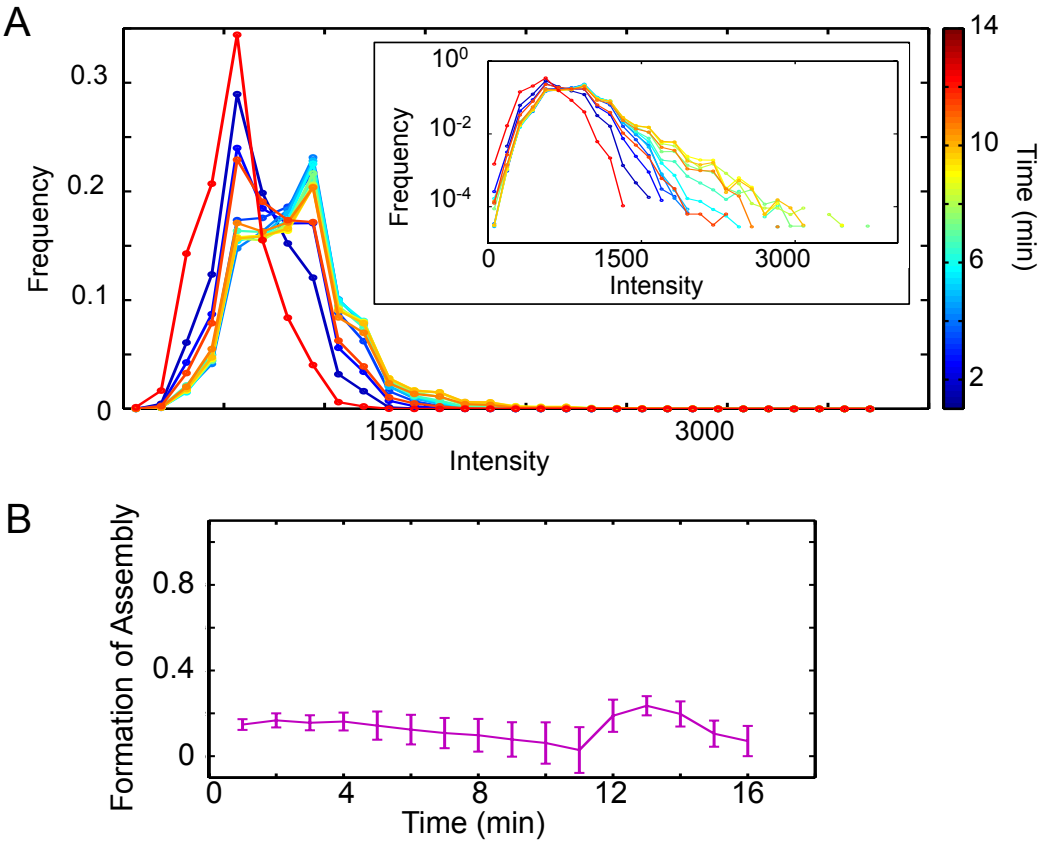

Figure S1. A. Related to Figure 4. The distribution of intensities over time at n.c. 13 for RFP-Fib fluorescent signal of a representative embryo. The inset shows the frequencies of intensities in the logarithmic scale, highlighting that the distributions develop a tail toward higher intensities in the middle time-points. Time zero marks the end of mitosis. **B.** For GFP-NLS, which does not form subnuclear assemblies, the calculated formation of assembly, as measured by the tail in the histogram of intensities (**A**) does not change at n.c. 13 and has values consistent with RFP-Fib during early time-points of n.c. 13. Mean value ± SEM is shown for the nuclei in four embryos.

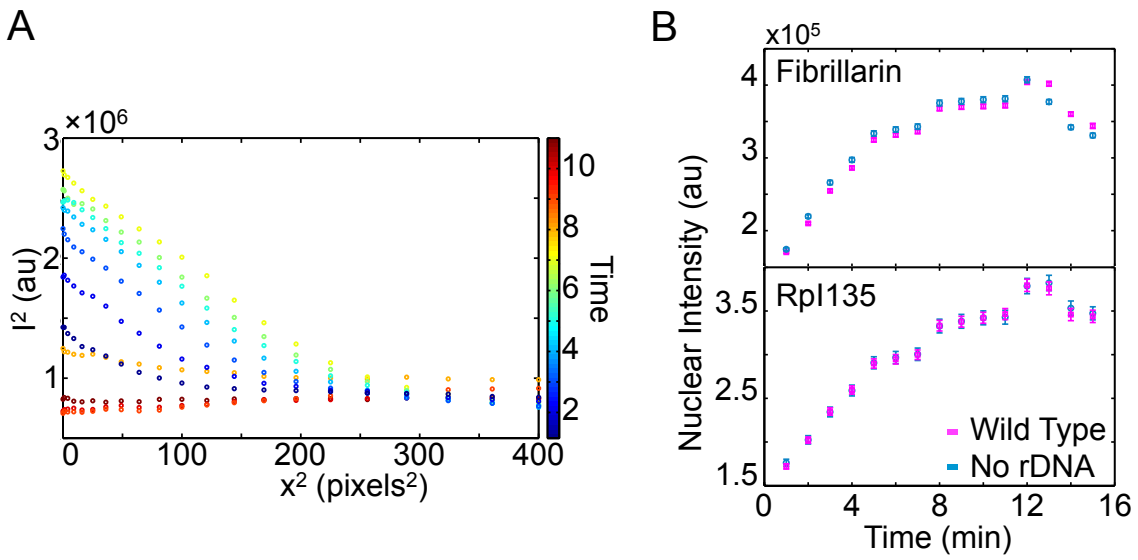

Figure S2. Related to Figure 5. **A.** Representative radial profiles of RFP-Fib nucleoplasmic signal averaged over all the nuclei in the field of view for a single embryo at n.c. 12. The slope of the linear part to the left is the dç. **B.** Total intensity per nucleus is depicted for RFP-Fib (top) and RpI135-GFP (bottom) as a function of time at n.c. 13 for the wild-type and mutant embryos lacking rDNA. Each point shows mean ± SEM (≈500 nuclei from 5 different embryos at each time-point). Time zero marks the end of mitosis.

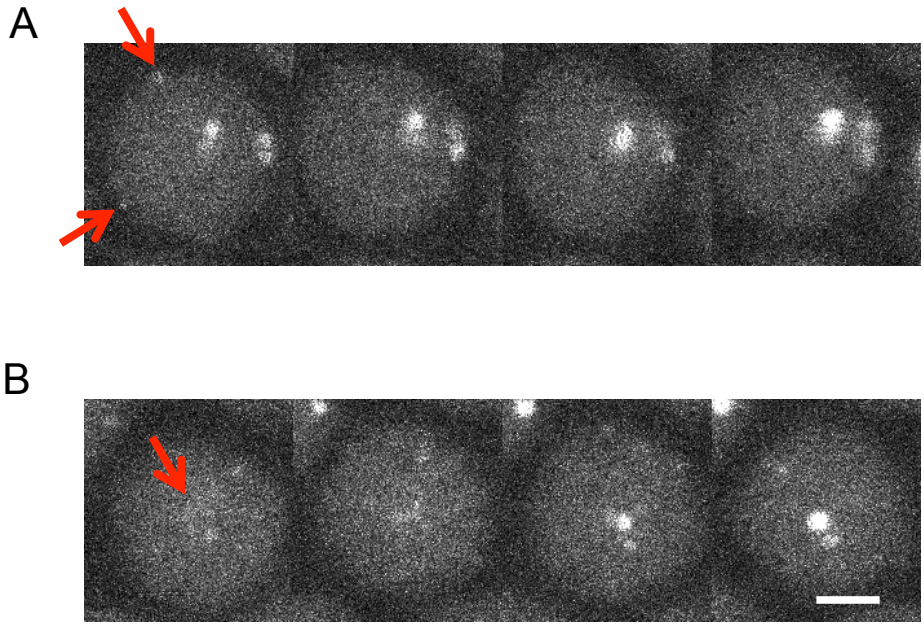

Figure S3. Related to Figure 6. The local inhomogeneities that appear at n.c. 14 either dissolve with the progression of interphase as shown in **A** with red arrows, or fuse to form the nucleolus (**B**). Scale bar is 2 μm. For the purpose of presentation, the images in have adjusted contrasts and changed saturation values.

SUPPLEMENTAL EXPERIMENTAL PROCEDURES

Detection of the nucleoli

All image analyses were performed with ImageJ (Rasband WS, ImageJ; National Institutes of Health; (1997–2008)) and MATLAB (MathWorks, Natick, MA) routines.

The nucleoli were detected using an automated image analysis algorithm applied on time-lapse confocal images of embryos expressing RFP-Fib and RpI135-GFP. We define nucleolus formation as the time at which above-background concentrations of nucleolar proteins are observed for the first time at NORs. In order to detect the nucleoli at early time-points, we start the analysis of nucleoli at later time-points when they can be readily detected with high level of confidence and track them back to earlier time points of that nuclear cycle at which their detection is more challenging. For a high-concentration assembly detected at earlier stages to qualify as a nucleolus, it must have spatial continuity with the later definitive nucleolus (i.e., the amount that it has shifted away from a nucleolus detected at an adjacent frame must not exceed 1.5 μm).

Measuring nucleoplasmic concentrations

The nucleoplasmic concentration of RpI135-GFP and RFP-Fib is a function of the fluorescent intensity per unit volume of the nucleus. Due to the spherical shape of the nucleus, the fluorescent signal of each pixel in the 2D image will be a function of position and the optical features of the microscope. We capture the signal from the whole nucleus using 20× HC PL APO Gly NA 0.7 objective on a Leica SP5 laser-scanning confocal microscope, with a large pinhole of size 140 μm. Therefore the intensity of a uniformly distributed protein at each point on the 2D image would be a function of its radial distance from the center of the circle given by:

$$I^2 = 4\,R^2\,d\varsigma^2 - d\varsigma^2\,x^2 \quad (1)$$

where I is the intensity, $d\varsigma$ is the difference between the nucleoplasmic and cytoplasmic intensity per unit volume, R is the radius of the nucleus, and x is the radial distance from the center of the nuclear mask. This shows a linear relationship between I^2 and x^2, with the slope being $d\varsigma^2$ (Figure S2A). Summing the nucleoplasmic intensities per unit volume with $d\varsigma$, and normalizing it to its maximum value gives ς. To measure nucleoplasmic concentrations at nuclear cycles 13 and 14, we mask the nucleoli by applying a difference of Gaussian filter and thresholding.

For calculating the total nuclear intensity per nucleus, the total intensity of a circle with the radius determined with equation (1) was measured, and averaged over all nuclei in the field of view at each time point.

Measuring homogeneity in the distribution of proteins

Embryos were imaged using 63× HCX PL APO CS 1.4 NA oil-immersion objective on a Leica SP5 laser-scanning confocal microscope equipped with GaAsP 'HyD' detectors, with pixels of 40 × 40 nm and z spacing of 2 μm. Maximum projected images were used for measuring the homogeneity. Homogeneity in the pixel intensities were measure by a customized GLCM method [S1]. To reduce the effect of noise, the average intensity of neighboring pixels was used. Boxes of different lengths were used to evaluate the effect of averaging on the results. The results become insensitive to the box size for boxes of 5 x 5 pixels or larger. This is equivalent to 200nm, which is close to the diffraction limit. The bin sizes for making the matrices were kept constant at different time points for consistency. The homogeneity was measured using the following equation:

$$Homogeneity = \sum_{i,j} \frac{p(i,j)}{1 + |i - j|}$$

where i and j are the centers of intensity bins, and $p(i,j)$ is the probability of two particular intensities being neighbors.

Transgenic lines

His2Av-GFP line was provided by the Bloomington Drosophila Stock Center. RpI135-GFP transgenic line is previously reported [S2]. For RFP-Fib line, a 2.25 Kb fragment including *D. melanogaster* genomic sequence of the *fibrillarin* gene with a *Drosophila* codon-optimized TagRFP-T and a linker inserted before the start of the gene was synthesized by GenScript and cloned into the pBabr vector. The resulting construct was then inserted into the *attP40* landing site in the *Drosophila* genome. Transgenic injections were performed by Genetic Services Inc. (Cambridge, MA). Primer and transgene sequences are available upon request.

Fly stocks and genetics

Fly stocks and crosses were maintained by standard methods at room temperature. Embryos expressing RFP-Fib and RpI135-GFP were obtained by crossing RFP-Fib/RpI135-GFP virgin females into OreR males. Unfertilized embryos were produced by crossing st^1 $\beta Tub85D^D$ ss^1 e^s/TM3, Sb males to OreR virgin females. $bTub85D^D$ is a

male-sterile allele and was obtained from the Bloomington Stock P{neoFRT}82B P{ovoD1-18}3R/st^{1} βTub85D^{D} ss^{1} e^{s}/TM3, Sb. C(1)DX / 0 embryos were obtained by crossing C(1)DX/Y^{Bs}; RFP-Fib/RpI135-GFP virgins to C(1;Y)*, y^{1} w^{a}/0 males. C(1)DX structurally lacks the nucleolus organizer regions [S3, S4]. 50 embryos from this cross are imaged as described above, and genotypes are scored based on the number and intensity of high concentration assemblies of RNA pol I and fibrillarin as described in [S2]. 25% of embryos in this cross are unambiguously scorable as C(1)DX / 0 and are operationally defined as the set of embryos that demonstrate weak or near-absent RNA pol I foci at n.c. 13 (e.g. Figure 4A, lower right panel).

Heat and formaldehyde fixation

Embryos were formaldehyde-fixed for *in situ* hybridization. Heat- and formaldehyde-fixation protocols were performed as described previously [S5], with slight modification to the formaldehyde-fixation technique in that the fixative used was 4% paraformaldehyde in PBS buffer.

FISH and immunofluorescence

In situ hybridization was performed using Dig-ITS1 probes at a concentration of 1 ng/µl. Standard digoxigenin-labeled RNA *in situ* hybridization was performed. The Dig-ITS1 probe was detected using an anti-Dig mouse primary antibody (1:250; Roche #11333062901) and an anti-mouse Alexa-647 secondary antibody (1:250; Molecular Probes, Eugene, OR).

Embryos were washed with PBT (PBS + 0.1% Triton-100), blocked with Blocking Buffer (10% BSA) for 1 hour, incubated with primary antibodies at 4°C overnight, washed 3x10 minutes with PTw (PBS + 0.1% Tween 20), incubated with secondary antibodies for two hours, washed 3x10 minutes with PTw, stained with DAPI for 3 minutes, and then washed 4x10 minutes with PTw. Hybridized and stained embryos were left in PTw in a 4°C refrigerator until mounted on slides. All steps were done at room temperature unless otherwise specified. Sequences for the primers are available upon request.

The primary antibody used for immunostaining was anti-Fibrillarin rabbit (1:100; Abcam, #5821), and the secondary antibody used was Alexa-647 anti-rabbit IgG (1:250; Molecular Probes, Eugene, OR). Imaging of the fixed embryos was performed at ~23°C with a Leica SP5 confocal microscope using a HCX PL APO lambda blue 63x/1.40 oil-immersion objective (Leica).

Single embryo qRT-PCR

Single embryos were precisely timed and used for qRT-PCR as described before [S2]. Primers of 5'ETS [S6], Tubulin, and RpI12 were used and their sequences are available upon request.

Quantification of the formation of assemblies

Embryos were imaged using 20× HC PL APO Gly NA 0.7 objective on a Leica SP5 laser-scanning confocal microscope. To measure the formation of assemblies (nucleoli or HANPs), nuclei were detected using a difference of Gaussian filter and thresholding, and the histogram of the intensities for each time-point were obtained for each embryo. As can be seen in Figure S1A, the distribution of the fluorescent intensities becomes more asymmetric with the progression of interphase. Accordingly, we use skewness as an unbiased measure of the formation of high-concentration assemblies:

$$Skewness = \frac{m_3}{s^3}$$

where m_3 is third moment and s is the standard deviation of the samples. For a control protein, GFP-NLS, that does not form assemblies, this measure remains unchanged and similar to values for RFP-Fib during early time-points of n.c. 13 (Figures 4F and S1B).

Quantification of the size of assemblies

Embryos were imaged using 63× HCX PL APO CS 1.4 NA oil-immersion objective on a Leica SP5 laser-scanning confocal microscope equipped with GaAsP 'HyD' detectors, with pixels of 40 × 40 nm and z spacing of 2 µm. To avoid variability due to photobleaching, the same number of time steps were imaged and compared. The assembly size in the mutants lacking rDNA was compared to other progeny of the same cross in which the nucleolus would form. By applying a difference of Gaussian filter and thresholding we generated an assembly mask, which was then used to measure the total intensity of assemblies per nucleus in the images taken. The same threshold value was used for different images.

Injection of RNAi

RNAi against RpI12 and RpI135 were prepared using PCR products containing T7 promoters (primers available upon request) as template for *in vitro* transcription using MEGAscript T7 Transcription kit (Invitrogen). The RNAi was injected into the embryo prior to n.c. 10 and imaged using 20× HC PL APO Gly NA 0.7 objective on a Leica SP5 laser-scanning confocal microscope.

SUPPLEMENTAL REFERENCES

S1. Haralick, R. M., Shanmugam, K., and Dinstein, I. (1973). Textural Features for Image Classification. IEEE Trans. Syst. Man. Cybern. *3*, 610–621.

S2. Blythe, S. A., and Wieschaus, E. F. (2015). Zygotic Genome Activation Triggers the DNA Replication Checkpoint at the Midblastula Transition. Cell *160*, 1169–1181.

S3. Muller, H. J. (1943). A stable double X chromosome. Drosoph. Inf. Serv. *17*, 61–62.

S4. Ritossa, F. M., and Spiegelman, S. (1965). Localization of DNA Complementary to Ribosomal RNA in the Nucleolus Organizer Region of Drosophila melanogaster. Proc. Natl. Acad. Sci. U. S. A. *53*, 737–45.

S5. Müller, H. A., and Wieschaus, E. (1996). armadillo, bazooka, and stardust are critical for early stages in formation of the zonula adherens and maintenance of the polarized blastoderm epithelium in Drosophila. J. Cell Biol. *134*, 149–63.

S6. Guerrero, P. a, and Maggert, K. a (2011). The CCCTC-Binding Factor (CTCF) of Drosophila Contributes to the Regulation of the Ribosomal DNA and Nucleolar Stability. PLoS One *6*, e16401.